

Neural network architecture for artifacts detection in ZTF survey

Timofey Semenikhin^{1,2}

¹ Lomonosov Moscow State University, Sternberg astronomical institute,
Universitetsky pr. 13, Moscow 119234, Russia

² Faculty of Space Research, Lomonosov Moscow State University, Leninsky Gori 1
bld. 52, Moscow 119234, Russia

Abstract. Today, astronomers are faced with the challenge of handling vast volumes of data, as modern instruments are capable of generating terabytes of data in a single night. One such instrument is the Zwicky Transient Facility, an automated sky survey that can detect approximately a million candidate astrophysical objects among the observed regions of the night sky in a single night. However, a significant portion of the detected objects turn out to be artifacts, i.e., phenomena with non-astrophysical origins. Therefore, specialists must invest time in manually classifying these objects, as there is currently no efficient method that can perform this task without human intervention. The goal of this work is the development of an algorithm to predict whether the light curve from the Zwicky Transient Facility data releases has a bogus nature or not based on the sequence of frames. A labeled dataset provided by experts was utilized, comprising 2230 frames series. Due to the substantial size of the frame sequences, the application of a variational autoencoder was deemed necessary for mapping the images into lower-dimensional vectors. For the task of binary classification based on sequences of compressed frame vectors, a recurrent neural network was employed. Several neural network models were considered, and the quality metrics were assessed using k-fold cross-validation. The final performance metrics, including ROC – AUC = 0.869 ± 0.016 and Accuracy = 0.804 ± 0.021 , suggest that the model has practical utility. The code implementing the algorithm is available on [GitHub](#).

Keywords: Neural network · Data analysis · Real-bogus classification.

1 Introduction

Zwicky Transient Facility (ZTF [1], [2]) is an automated sky survey. The telescope generates a large amount of data every night. The survey data consists of images capturing specific parts of the sky, which are later used to create data releases (DRs).

The purpose of creating data releases is to investigate any variable sources in the sky. The survey frames are processed using the widely-used algorithm

SExtractor [3], which detects sources and performs photometry on them. Subsequently, all variable sources are assigned a unique object ID (OID), which is added to the so-called ZTF data releases. It is assumed that there should be no non-periodic variable objects (such as supernovae, red dwarf flares, etc.) in the DRs. However, due to the fact that the applied algorithms are not perfect, unusual objects are encountered in this data [8,10,4]. This motivates researchers, even those whose scientific interests are not related to variable stars, to work with DRs.

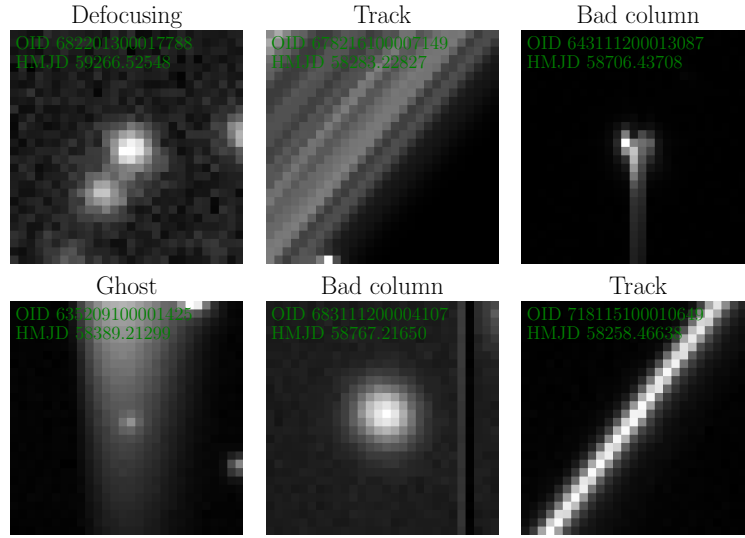


Fig. 1. Examples of artifacts found within ZTF data. Images size is 28x28 pixels.

Unfortunately, among the ZTF data, so-called artifacts are often encountered (see Fig. 1). An artifact is commonly referred to as any phenomenon of non-astrophysical nature. These can be effects related to instrument malfunction (defocusing, saturated columns in the CCD array, etc.) or effects associated with external conditions (atmospheric turbulence, clouds, bright satellites, etc.). Under certain circumstances, these phenomena can be classified as astrophysical objects by machine learning methods, which significantly complicates working with ZTF data.

Classifying astrophysical objects is one of the primary and most challenging tasks when working with DR data because they lack class labels. As a result, instead of directly using a sequence of object images, photometric observations are often employed. Since the observational properties of many astrophysical classes have been sufficiently studied, a set of features can be derived from the light curve (temporal sequence of photometric observations) that allows for their differentiation. Subsequently, classification methods from classical machine learning can

be applied to the constructed feature sets to solve the classification task. However, this approach can lead to situations where astrophysical phenomena and artifacts closely resemble each other in their photometric representation. For example, a passing bright satellite may temporarily illuminate a specific region of the detector, which can be mistaken for a brief flare of a red dwarf, appearing as a short-lived peak in the light curve. Therefore, when tackling such problems, specialists need to spend time validating the obtained results. Artifacts can account for 68% of the total number of objects labeled as astrophysical objects by machine learning methods [8].

This work is dedicated to implementing an algorithm that would avoid the involvement of specialists in classifying artifact/non-artifact objects from DR. Currently, there is no efficient approach that solves this problem.

2 Data

The labeled object dataset was taken from the SNAD Viewer [9] web portal³. Each object has a unique index, OID, and a set of labels indicating whether it is an artifact or not, along with additional details about the nature of the object (e.g., AGN – active galactic nucleus, variable, etc. Similarly, for artifacts: ghost, defocusing, etc.). For each object, there is a series of telescope images captured at different times. To obtain a list of links to all available images for a given OID, an API service⁴ is used.

A telescope frame is an image of size 3072x3080 depicting a portion of the sky. However, for this task, only a small area within this frame, associated with a specific object, is of interest. Thus, images are cropped to a size of 28x28 pixels and normalized.

The dataset contains 2230 objects (image series), including 1150 artifacts and 1080 astrophysical objects, totaling 1,015,177 images.

One of the main challenges of the task is that objects have a large number of observations (see Fig. 2), and it is unknown at which specific time points anomalies were observed. Therefore, an algorithm capable of working with sequences of images rather than individual anomalous images is necessary.

3 Methods

The implemented approach involves two stages. First, a variational autoencoder (VAE) is trained on all images in the dataset to obtain informative compressed representations of frames. Then, a recurrent neural network (RNN) is trained on sequences of these compressed representations to solve the classification task. Combining these two stages into a single recurrent neural network with convolutional layers at the beginning is not feasible due to computational resource limitations. All neural networks are implemented using the Python library PyTorch.

³ <https://ztf.snad.space/>

⁴ http://finder.fits.ztf.snad.space/api/docs#operation/Get_URLs_for_all_exposures_by_object_ID_api_v1_urls_by_oid_get

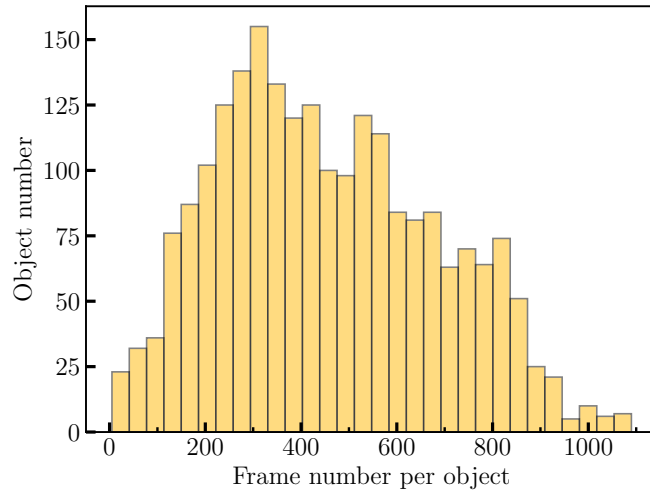


Fig. 2. Distribution of images number per object.

3.1 Variational autoencoder

The implemented encoder consists of 5 convolutional layers (with image channel dimensions: 32, 64, 128, 256, 512 respectively) with the LeakyReLU activation function and batch normalization after each layer. Each output convolutional layer returns half the size of the input image, so the encoder output is a vector, whose size is a model parameter. The architecture of the decoder is symmetrical to that described above, except that transposed convolutional layers are used instead of convolutional layers.

The VAE was trained on all images from dataset. When selecting the parameters for the VAE, different levels of image compression were considered. In machine learning literature, the vector obtained at the output of the encoder is commonly referred to as the latent state. In Fig. 3, the blue and green lines represent the loss curves for latent state sizes of 36 and 78, respectively. It can be observed that increasing the latent state size requires more training epochs. In this work, a latent state size of 36 proved to be optimal. Image augmentation through random rotation was also explored (red line in Fig. 3); however, it was found that this significantly increased the number of required training epochs without a visible improvement in the model. Therefore, the final model does not include any augmentations. For model training, the Adam [7] optimizer was used with a *learning rate* = $5 \cdot 10^{-5}$ for 100 epochs. The core idea of the Adam optimizer is to combine adaptive moment estimation with adaptive learning rates for efficient model optimization in machine learning. The loss function for the

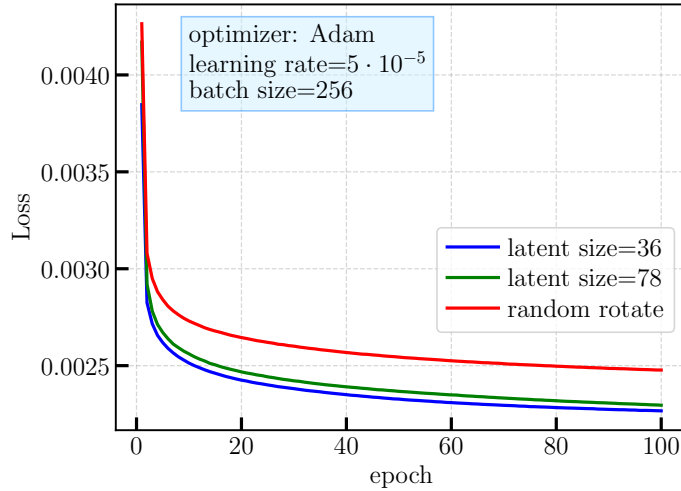


Fig. 3. Loss functions during training a VAE.

VAE takes the following form:

$$L = \text{LogCosh}(x, \hat{x}) + \omega_{kld} \cdot KL(N(\mu, \sigma) || N(0, 1)) = \ln \cosh(x - \hat{x}) + \omega_{kld} \cdot \left(\ln \frac{1}{\sigma} + \frac{\sigma^2 + \mu^2}{2} - \frac{1}{2} \right), \quad (1)$$

here, x, \hat{x} represent the original image and its reconstruction by the decoder, respectively; μ, σ are vectors of means and variances obtained from the encoder's output; $\omega_{kld} = 8 \cdot 10^{-5}$ serves as the weight coefficient for the Kullback-Leibler divergence.

By using the compressed representations of the images, it is expected that the compressed representations of anomalous frames are outliers from the overall distribution of normal images. After the VAE was trained, the obtained compressed representations of frames were saved. The next stage of the work involved training a RNN for binary classification.

3.2 Recurrent neural network

The fundamental idea behind RNNs is the utilization of hidden states that capture information from previous time steps, allowing them to maintain a form of memory and learn dependencies within sequential data. By using recurrent connections, RNNs can model sequences of arbitrary length, making them powerful tools for tasks involving sequential information. However, traditional RNNs have issues with vanishing and exploding gradients, leading to difficulties in learning long-range dependencies. To address this, various RNN architectures like LSTM (Long Short-Term Memory; [6]) and GRU (Gated Recurrent Unit; [5]) have

been developed, which introduce gating mechanisms to better control the flow of information and mitigate gradient-related problems.

The model takes inputs of size [batch size, sequence length, latent_dim], where latent_dim represents the dimensionality of the compressed representation. Embeddings for object frames, along with their corresponding class labels, are fed into a RNN. The model parameters are optimized using the Adam optimizer with a *learning rate* = 10^{-4} for 500 epochs.

Table 1. Model results. The metric values are averaged over 5 test folds, as well as the standard deviation.

Model name	ROC-AUC	Accuracy	F1-score
GRU	0.825 ± 0.061	0.751 ± 0.073	0.775 ± 0.046
bidirectional GRU + L_2	0.869 ± 0.016	0.804 ± 0.021	0.809 ± 0.015
GRU + Tversky loss	0.839 ± 0.027	0.776 ± 0.037	0.786 ± 0.019
LSTM	0.725 ± 0.085	0.706 ± 0.098	0.742 ± 0.035

The baseline model considered was a GRU layer with a hidden state size of 128, and the loss function used during training the recurrent neural network was cross-entropy. In addition to the baseline model, the following variations were explored: a bidirectional GRU cell with L_2 weight regularization (*weight decay* = 10^{-5}); a GRU layer with a modified loss function (the Tversky Index [11]) term was added to the loss function); a LSTM layer with the same parameters as the baseline model.

Bidirectional GRU is different from the regular GRU in that it processes input sequences in both forward and backward directions, which enables it to capture contextual information from past and future time steps. However, when using such an approach in this task, the model experienced overfitting, so L_2 weight regularization was added to it. The table 1 shows the main results for the considered models. The best result is achieved with a bidirectional GRU layer with L_2 weight regularization.

4 Conclusions

Throughout the course of this study, sequences of ZTF object frames from a labeled dataset were downloaded and preprocessed. Using the PyTorch library, a variational autoencoder was implemented and trained, enabling the compression of images into informative lower-dimensional vectors. Several models of recurrent neural networks were considered for the task of binary classification based on sequences of compressed image vectors. The quality metrics of the models were evaluated using k-fold cross-validation, with the best-performing model achieving

an ROC – AUC = 0.869 ± 0.016 and Accuracy = 0.804 ± 0.021 . All the code used in the study is available on [GitHub](#)⁵.

Thus, an algorithm has been developed that aims to classify objects from ZTF DR in a manner similar to that of a specialist who annotated the training dataset. This algorithm stands out from others by utilizing sequences of observation frames rather than photometric time series. While computationally more challenging, images contain more information about the object’s radiation than its corresponding photometry.

The next stage of the work will involve: searching for the optimal architecture for both the autoencoder and the recurrent network; selecting the most effective loss function for the classifier in terms of our task; analyzing the dependence of the first and second type errors on the chosen threshold value; conducting computational experiments using different optimizers. This algorithm can be employed within the scope of the SNAD⁶ project, as the obtained quality metrics indicate its practical value. Since the training dataset used in this work was annotated by specialists from the SNAD project, it is expected that the implementation of this algorithm into the general pipeline will reduce the number of artifacts among anomalies. This will enable specialists to detect more new astrophysical objects.

Acknowledgements The author thanks the SNAD team for the provided comments and support. The author acknowledges the support of M.V. Lomonosov Moscow State University Program of Development. Supported by Nonprofit Foundation for the Development of Science and Education “Intellect”.

References

1. Bellm, E.C., Kulkarni, S.R., Barlow, T., Feindt, U., Graham, M.J., Goobar, A., Kupfer, T., Ngeow, C.C., Nugent, P., Ofek, E., Prince, T.A., Riddle, R., Walters, R., Ye, Q.Z.: The Zwicky Transient Facility: Surveys and Scheduler. **131**(1000), 068003 (Jun 2019). <https://doi.org/10.1088/1538-3873/ab0c2a>
2. Bellm, E.C., Kulkarni, S.R., Graham, M.J., Dekany, R., Smith, R.M., Riddle, R., Masci, F.J., Helou, G., Prince, T.A., Adams, S.M., Barbarino, C., Barlow, T., Bauer, J., Beck, R., Belicki, J., Biswas, R., Blagorodnova, N., Bodewits, D., Bolin, B., Brinnel, V., Brooke, T., Bue, B., Bulla, M., Burruss, R., Cenko, S.B., Chang, C.K., Connolly, A., Coughlin, M., Cromer, J., Cunningham, V., De, K., Delacroix, A., Desai, V., Duev, D.A., Eadie, G., Farnham, T.L., Feeney, M., Feindt, U., Flynn, D., Franckowiak, A., Frederick, S., Fremling, C., Gal-Yam, A., Gezari, S., Giomi, M., Goldstein, D.A., Golkhou, V.Z., Goobar, A., Groom, S., Hacopians, E., Hale, D., Henning, J., Ho, A.Y.Q., Hover, D., Howell, J., Hung, T., Huppenkothen, D., Imel, D., Ip, W.H., Ivezić, Ž., Jackson, E., Jones, L., Juric, M., Kasliwal, M.M., Kaspi, S., Kaye, S., Kelley, M.S.P., Kowalski, M., Kramer, E., Kupfer, T., Landry, W., Laher, R.R., Lee, C.D., Lin, H.W., Lin, Z.Y., Lunnan,

⁵ https://github.com/semim/RB_ZTF

⁶ <https://snad.space/>

- R., Giomi, M., Mahabal, A., Mao, P., Miller, A.A., Monkewitz, S., Murphy, P., Ngeow, C.C., Nordin, J., Nugent, P., Ofek, E., Patterson, M.T., Penprase, B., Porter, M., Rauch, L., Rebbapragada, U., Reiley, D., Rigault, M., Rodriguez, H., van Roestel, J., Rusholme, B., van Santen, J., Schulze, S., Shupe, D.L., Singer, L.P., Soumagnac, M.T., Stein, R., Surace, J., Sollerman, J., Szkody, P., Taddia, F., Terek, S., Van Sistine, A., van Velzen, S., Vestrand, W.T., Walters, R., Ward, C., Ye, Q.Z., Yu, P.C., Yan, L., Zolkower, J.: The Zwicky Transient Facility: System Overview, Performance, and First Results. **131**(995), 018002 (Jan 2019). <https://doi.org/10.1088/1538-3873/aacbe>
3. Bertin, E., Arnouts, S.: SExtractor: Software for source extraction. **117**, 393–404 (Jun 1996). <https://doi.org/10.1051/aas:1996164>
 4. Chan, H.S., Villar, V.A., Cheung, S.H., Ho, S., O’Grady, A.J.G., Drout, M.R., Renzo, M.: Searching for anomalies in the ztf catalog of periodic variable stars. *The Astrophysical Journal* **932**(2), 118 (jun 2022). <https://doi.org/10.3847/1538-4357/ac69d4>, <https://dx.doi.org/10.3847/1538-4357/ac69d4>
 5. Cho, K., van Merriënboer, B., Gulcehre, C., Bahdanau, D., Bougares, F., Schwenk, H., Bengio, Y.: Learning phrase representations using rnn encoder-decoder for statistical machine translation (2014)
 6. Hochreiter, S., Schmidhuber, J.: Long Short-Term Memory. *Neural Computation* **9**(8), 1735–1780 (11 1997). <https://doi.org/10.1162/neco.1997.9.8.1735>, <https://doi.org/10.1162/neco.1997.9.8.1735>
 7. Kingma, D.P., Ba, J.: Adam: A method for stochastic optimization (2017)
 8. Malanchev, K.L., Pruzhinskaya, M.V., Korolev, V.S., Aleo, P.D., Kornilov, M.V., Ishida, E.E.O., Krushinsky, V.V., Mondon, F., Sreejith, S., Volnova, A.A., Belinski, A.A., Dodin, A.V., Tatarnikov, A.M., Zheltoukhov, S.G., (The SNAD Team): Anomaly detection in the Zwicky Transient Facility DR3. **502**(4), 5147–5175 (Apr 2021). <https://doi.org/10.1093/mnras/stab316>
 9. Malanchev, K., Kornilov, M.V., Pruzhinskaya, M.V., Ishida, E.E.O., Aleo, P.D., Korolev, V.S., Lavrukhina, A., Russeil, E., Sreejith, S., Volnova, A.A., Voloshina, A., Krone-Martins, A.: The snad viewer: Everything you want to know about your favorite ztf object. *Publications of the Astronomical Society of the Pacific* **135**(1044), 024503 (feb 2023). <https://doi.org/10.1088/1538-3873/acb292>, <https://dx.doi.org/10.1088/1538-3873/acb292>
 10. Pruzhinskaya, M.V., Ishida, E.E.O., Novinskaya, A.K., Russeil, E., Volnova, A.A., Malanchev, K.L., Kornilov, M.V., Aleo, P.D., Korolev, V.S., Krushinsky, V.V., Sreejith, S., Gangler, E.: Supernova search with active learning in ZTF DR3. **672**, A111 (Apr 2023). <https://doi.org/10.1051/0004-6361/202245172>
 11. Salehi, S.S.M., Erdogmus, D., Gholipour, A.: Tversky loss function for image segmentation using 3d fully convolutional deep networks (2017)

Dear Editors,

Please, find below our replies to the referee's comments. Also, all the changes are implemented to the manuscript.

Additionally, we've updated the author list and acknowledgements.

SUBMISSION: 71

TITLE: Neural network architecture for artifacts detection in ZTF survey

----- **REVIEW 1** -----

----- Overall evaluation -----

SCORE: 3 (strong accept)

----- TEXT:

The Zwicky Transient Facility (ZTF) is the largest (at least in terms of the instrument's field of view) photometric survey of the sky.

ZTF provides information about variable celestial objects/phenomena, but also contains a number of artifacts that are not astronomical objects.

The authors of the reviewed paper have developed a methodology for searching for artifacts, which, obviously, will be in demand by researchers dealing with ZTF data.

The authors write that their dataset contains 1,150 artifacts and 1,080 astronomical objects.

Comment 1:

1) It would be useful to indicate how much these numbers correspond to the actual ratio of the number of artifacts to the number of real objects in ZTF.

Reply:

Unfortunately, the actual ratio of artifacts to non-artifacts within the ZTF survey data releases is unknown as they are not labeled. Latest data release of ZTF contains ~4.72 billion light curves. Such a huge amount of information can not be processed manually, this is one of the reasons why the use of machine learning algorithms becomes unavoidable.

----- **REVIEW 2** -----

----- Overall evaluation -----

SCORE: 1 (weak accept)

----- TEXT:

The paper describes the developed algorithm that predicts whether a sequence of object images from the Zwicky Transient Facility survey is an artifact or not. The proposed method consists of two parts: building a variational autoencoder and implementing a recurrent neural network. Both parts are described. The experiment used a labeled dataset, consisting of 2230 objects, approximately half of which are artifacts. The obtained results are presented in the paper. Some implementations of recurrent neural network (RNN) were considered. It was demonstrated that the best result (ROC - AUC = 0.869 ± 0.016 and Accuracy = 0.804 ± 0.021) was obtained with a bidirectional GRU cell with L2 weight regularization.

The paper describes one concrete algorithm for solving rather specific task.

The paper is clear, decently written and can be accepted as a short message.

----- **REVIEW 3** -----

----- Overall evaluation -----

SCORE: 3 (strong accept)

----- TEXT:

Статья написана на актуальную тему использования данных больших обзоров для классификации объектов с помощью сверхточных нейронных сетей (СНН). В частности, СНН используется для проверки классификации переменных объектов, уже обнаруженных пакетом SExtracor и полученных фотометрических рядах тем же пакетом.

Конкретная цель статьи – сообщение о процессе разработки алгоритма, предсказывающего, является ли последовательность изображений объектов из исследования Zwicky Transient Facility артефактом или нет.

Основные замечания

Комментарий 1:

1) «Since the methods used in processing ZTF data cannot guarantee absolute accuracy, artifacts can occur.»

Необходимо уточнить, о какой точности идет речь. Более точно, термин точность здесь не применим. Применим термин фатальная ошибка калибровки или фотометрии, или построения кривой блеска. Как правило, артефакты наблюдения (космические лучи, горячие пиксели итп. устраняются калибровкой и пользователи каталогов не подозревают о их существовании. Если же авторы берут для повторной обработки изображения, то эти изображения уже все откалиброваны. Поэтому стоит пояснить что именно является артефактом для авторов

Ответ:

Предложение изменено на: “Unfortunately, among the ZTF data, so-called artifacts are often encountered (see Fig.1).”

Как показывает наш анализ, в каталогах ZTF содержится большое количество артефактов наблюдения, включая космики, пролеты спутников и т.д.: часть из них приведена в каталоге артефактов SNAD (<https://snad.space/art/>).

В статье добавлен рисунок с примерами встречающихся артефактов.

Комментарий 2:

2) Статья ссылается на методы, и результаты без объяснения деталей. Было бы уместным более детально сказать в нужных местах о смысле метода или алгоритма, если метода или алгоритма не является общепринятым.

Ответ:

В секции 3.1 добавлено пояснение для Adam, а также более подробно описана работа с вариационным энкодером.

В секции 3.2 добавлены пояснения для GRU, LSTM.

Комментарий 3:

3) Абстракт.

«Целью данной работы является разработка алгоритма, предсказывающего, является ли последовательность изображений объектов из исследования Zwicky Transient Facility артефактом или нет.»

Последовательность изображений не может являться артефактом. Необходимо скорректировать это предложение. Видимо, сами объекты на изображениях могут являться артефактами.

Ответ:

Предложение исправлено на “The goal of this work is the development of an algorithm to predict whether the light curve from the Zwicky Transient Facility data releases has a bogus nature or not, based on the sequence of frames”

Комментарий 4:

4) For example, a passing bright satellite may temporarily illuminate a specific region of the detector, which can be mistaken for a brief flare of a red dwarf, appearing as a short-lived peak in the light curve.

При типичной экспозиции ZTF 30-60 сек, прохождение низкоорбитального КА в поле зрения телескопа приводит к появлению полосы на кадре. Не очень понятно как полоса может быть принята за вспышку. Более того, есть методы, которые выделяют и устраняют именно такие полосы на кадрах.

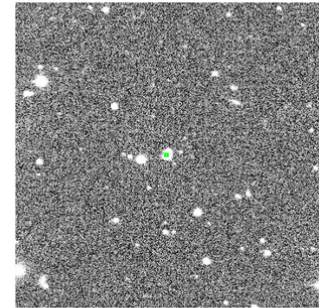
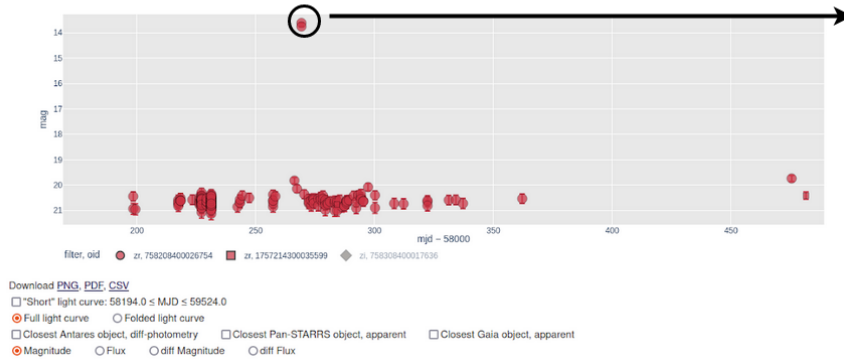
Ответ:

К сожалению, среди данных ZTF встречаются такие артефакты (в статью добавлен рисунок с примерами найденных артефактов – Fig.1). Фотометрические ряды, представленные в ZTF, реальных вспышек и полос могут быть очень похожи друг на друга (см. Рис.1 ниже).

SNAD ZTF DR17 object viewer

ZTF DR OID or SNAD name
Coordinates or name radius, arcsec

758208400026754

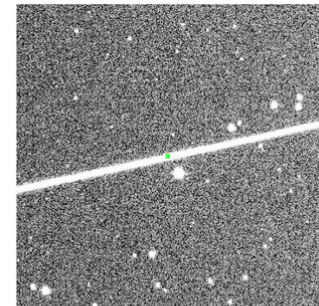
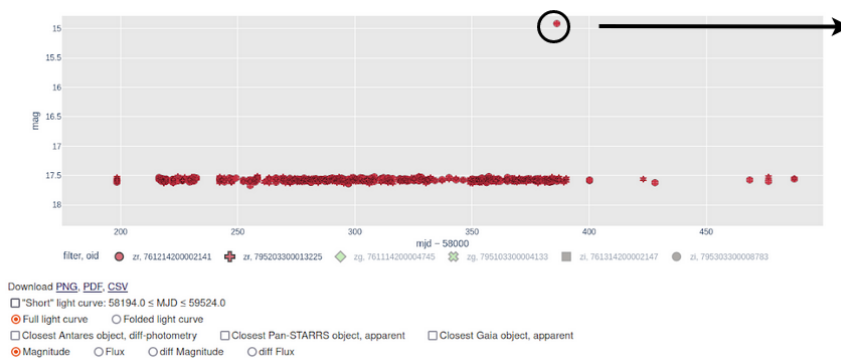


[Open in JS9](#) [Download FITS](#) [Product directory](#)

SNAD ZTF DR17 object viewer

ZTF DR OID or SNAD name
Coordinates or name radius, arcsec

761214200002141



[Open in JS9](#) [Download FITS](#) [Product directory](#)

Рис.1 Сверху: вспышка красного карлика. Снизу: артефакт на изображении - трек движущегося объекта.

Комментарий 5:

5) The labeled object dataset was taken from the SNAD Viewer⁴ web portal

В сноске 4 приведена ссылка на статью. Необходимо дать прямую ссылку на портал

Ответ:

Исправлено

Комментарий 6:

6) We considered several models based on the standard GRU layer.

Не определена аббревиатура GRU, не написано ничего про алгоритм Adam

Ответ:

В секции 3.2 добавлено пояснение для GRU и LSTM, а также добавлены ссылки на соответствующие статьи. В секции 3.1 добавлено описание для Adam и соответствующая ссылка.